AAOS
AMERICAN ACADEMY OF ORTHOPAEDIC SURGEONS

EXHIBIT SELECTION

# MRI of the Elbow: Techniques and Spectrum of Disease

## AAOS Exhibit Selection

Ashvin K. Dewan, MD, A. Bobby Chhabra, MD, A. Jay Khanna, MD, MBA, Mark W. Anderson, MD, and Lance M. Brunton, MD

*Investigation performed at the Department of Orthopaedic Surgery, The Johns Hopkins University, Baltimore, Maryland; the Departments of Orthopaedic Surgery and Radiology, University of Virginia, Charlottesville, Virginia; and the University of Pittsburgh School of Medicine, Pittsburgh, Pennsylvania*

**Background:** Magnetic resonance imaging (MRI) of the elbow allows for high-resolution evaluation of osseous and soft-tissue structures, including ligaments, tendons, nerves, and muscles. Multiple imaging techniques and pulse sequences exist. The purpose of this article is to update orthopaedic surgeons on current MRI techniques and illustrate the spectrum of elbow pathology detectable by MRI.

**Methods:** We searched MEDLINE with use of the keywords ''MRI'' and ''elbow'' for studies less than five years old evaluating MRI techniques. These papers, our experience, and textbooks reviewing elbow MRI provided the information for this article.

**Results:** We discuss the essentials and applications of the following techniques: (1) conventional, non-gadolinium-enhanced MRI; (2) gadolinium-enhanced MRI; and (3) magnetic resonance arthrography. The classic MRI appearances of occult fractures, loose bodies, ulnar collateral ligament injuries, lateral collateral ligament complex injuries, biceps tendon injuries, triceps tendon injuries, lateral epicondylitis, medial epicondylitis, septic arthritis, osteomyelitis, osteochondritis dissecans, compression neuropathies, synovial disorders, and various soft-tissue masses are reviewed.

**Conclusions:** MRI is a valuable, noninvasive method of elbow evaluation. This article updates orthopaedic surgeons on the various available MRI techniques and facilitates recognition of the MRI appearances of the most commonly seen pathologic elbow conditions.

## Imaging Sequences

The incorporation of dedicated surface coils and higher-strength magnets has improved magnetic resonance imaging (MRI) scanner quality, providing high-resolution imaging of the elbow with superb soft-tissue contrast. Elbow MRI is typically performed with the patient supine and the arm at the side, minimizing the rotation of the radioulnar joint relative to the humerus. By manipulating the scanning parameters when performing an MRI examination, contrast differences between tissues can be emphasized on the basis of

**Disclosure:** None of the authors received payments or services, either directly or indirectly (i.e., via his or her institution), from a third party in support of any aspect of this work. One or more of the authors, or his or her institution, has had a financial relationship, in the thirty-six months prior to submission of this work, with an entity in the biomedical arena that could be perceived to influence or have the potential to influence what is written in this work. No author has had any other relationships, or has engaged in any other activities, that could be perceived to influence or have the potential to influence what is written in this work. The complete **Disclosures of Potential Conflicts of Interest** submitted by authors are always provided with the online version of the article.

Fig. 1-A

Fig. 1-B

**Figs. 1-A and 1-B** Acute bone injuries. **Fig. 1-A** Occult fracture. A sagittal T2-weighted image of an occult radial head fracture. Radiographs were normal. Note the low-signal-intensity curvilinear fracture line (arrow) and surrounding edema. **Fig. 1-B** Bone contusions. A STIR image after a posterior elbow dislocation in this patient shows high signal intensity within the capitellum and radial head, indicative of marrow edema (arrows). No discrete low-signal-intensity fracture lines are evident. (Adapted from: J Hand Surg Am. 31[6]; Brunton LM, Anderson MW, Pannunzio ME, Khanna AJ, Chhabra AB; Magnetic resonance imaging of the elbow: update on current techniques and indications; p 1001-11; Copyright 2006; with permission from Elsevier.)

inherent tissue properties (T1 and T2), resulting in "T1-weighted" and "T2-weighted" images. T1-weighted images are best for illustrating anatomic detail, whereas T2-weighted images highlight alterations in water content. Short tau inversion recovery (STIR) and fat-suppressed T2-weighted images accentuate fluid and edema and are the most sensitive for detecting pathologic changes. Gradient-echo scanning is useful for other specialized applications[1].

The intravenous administration of a gadolinium-based contrast agent provides valuable information when evaluating soft-tissue masses and synovial disorders. Such a contrast agent is particularly useful for differentiating true cystic lesions from certain solid lesions. For soft-tissue infection, the peripheral enhancement of an abscess will often allow for its differentiation from adjacent purulent material. Striking synovial enhancement after contrast agent administration is helpful for diagnosing an inflammatory arthritis. Intravenous gadolinium contrast agent is also effective at demonstrating bone perfusion and viability[1].

Magnetic resonance arthrography (MRA) is indicated for intra-articular or periarticular pathologic conditions such as collateral ligament tears, capsular disruptions, osteochondritis dissecans, and loose bodies. A total of 5 to 10 mL of dilute gadolinium contrast agent is injected into the joint before image acquisition[1].

## Pathologic Conditions

### *Trauma*

#### Occult Fractures

Persistent tenderness over a suspected injury site without an abnormality on conventional radiographs may be an indication for MRI examination to detect an occult fracture. The posterior fat pad sign on conventional radiographs corresponds to the presence of an occult fracture in >75% of patients[1-3]. MRI may characterize the osseous injury when conventional radiographs appear normal. Fat-suppressed T2-weighted (or STIR) pulse sequences are the most sensitive for detecting occult traumatic or stress fractures[1]. True fractures will show a linear pattern of signal change, with decreased signal on T1-weighted images and/or increased signal on T2-weighted images (Fig. 1-A). In contrast, a bone contusion

Fig. 2

Epiphysiolysis (Little Leaguer's elbow). A coronal STIR image of the right elbow shows diffuse high signal intensity within the medial epicondyle, consistent with epiphysiolysis from repetitive valgus stress to the elbow (arrow). Note the normal UCL (arrowhead).

produces a nonspecific increase in signal without a discrete fracture line on T2-weighted images (Fig. 1-B).

The radial head is the most frequent site of occult fracture in the adult elbow[2]. The anterolateral portion of the radial head is devoid of cartilage and lacks a subchondral plate, predisposing it to fracture[4]. Radial head fractures are occasionally associated with ligament or capsular disruptions, loose bodies, and/or capitellar bone contusions.

In children with radiographic evidence of joint effusion, MRI is useful for physeal injury evaluation[1,5]. A common apophyseal injury seen in skeletally immature throwing athletes is Little Leaguer's elbow. Repetitive valgus stress across the elbow during throwing may produce epiphysiolysis at the medial epicondylar apophysis with widening of the growth cartilage and an increase in T2 signal intensity[6]. Little Leaguer's elbow is best evaluated with use of a physeal cartilage-sensitive pulse sequence such as a coronal fat-suppressed gradient-echo sequence (Fig. 2)[7,8].

### Loose Bodies

Intra-articular loose bodies generate pain with joint motion and are often accompanied by mechanical symptoms such as catching or locking. Conventional radiographs or computed tomography scans may detect the presence of osseous loose bodies in the elbow joint, but MRI is especially useful for detecting intra-articular cartilaginous or osteocartilaginous loose bodies[1]. Loose bodies, usually found in the olecranon or coronoid

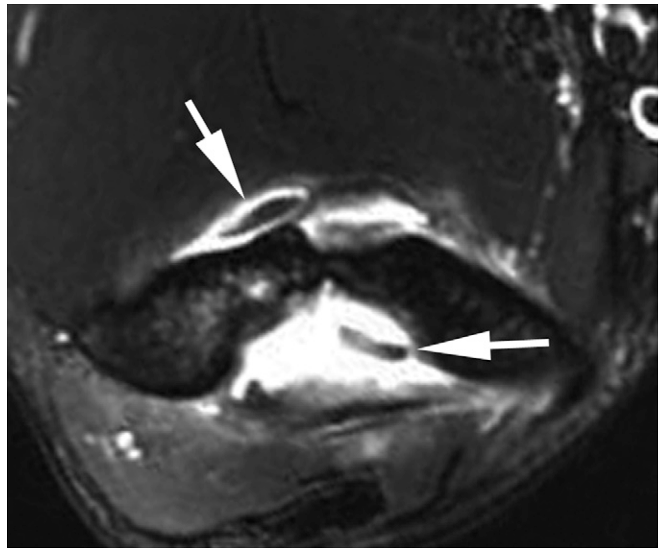

Fig. 3-A

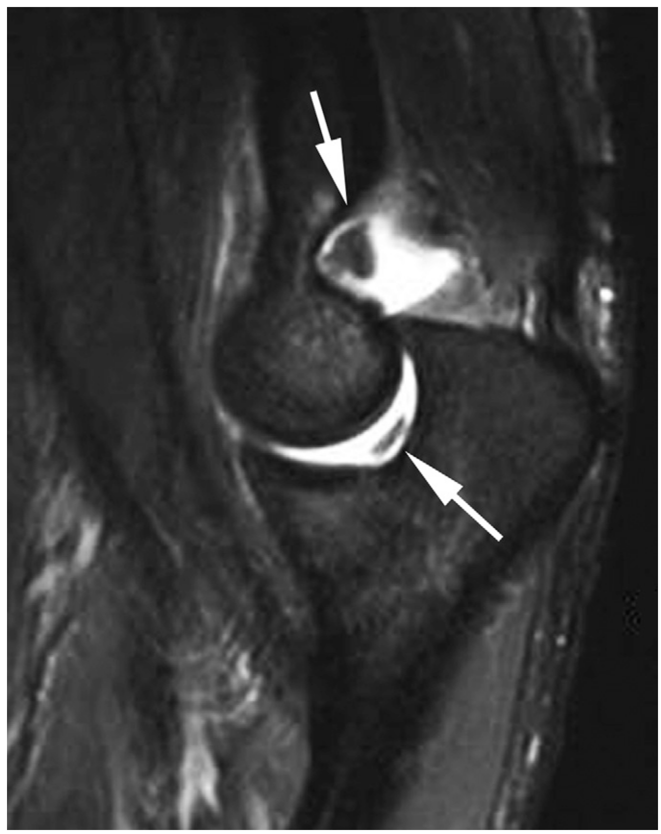

Fig. 3-B

**Figs. 3-A and 3-B** Loose bodies. (Adapted from: J Hand Surg Am. 31[6]; Brunton LM, Anderson MW, Pannunzio ME, Khanna AJ, Chhabra AB; Magnetic resonance imaging of the elbow: update on current techniques and indications; p 1001-11; Copyright 2006; with permission from Elsevier.) **Fig 3-A** An axial T2-weighted image shows loose bodies (arrows) in the sigmoid and olecranon fossae. **Fig. 3-B** A sagittal view of the same loose bodies (arrows).

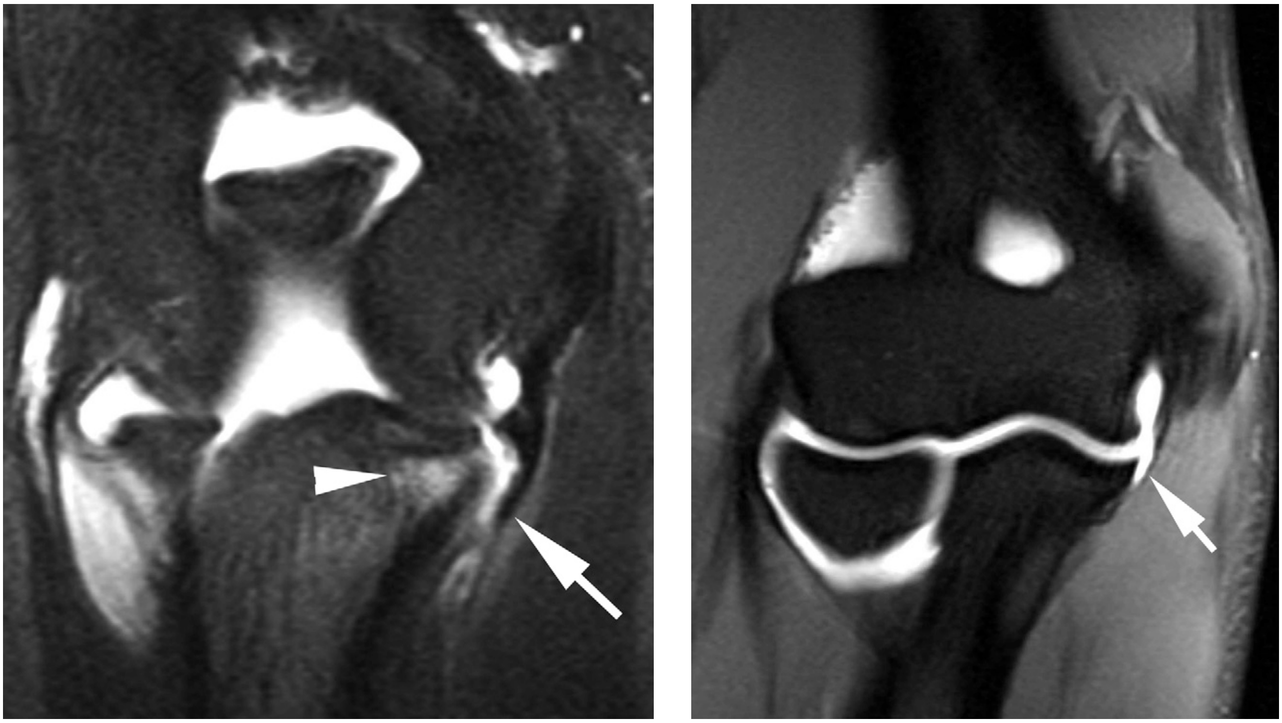

Fig. 4-A

Fig. 4-B

**Figs. 4-A and 4-B** UCL tears. **Fig. 4-A** Complete tear of the UCL. A coronal fat-suppressed T2-weighted image from an MR arthrogram shows discontinuity of the UCL at its distal attachment (arrow) with marrow edema in the sublime tubercle (arrowhead). **Fig. 4-B** Partial tear of the UCL. A coronal fat-suppressed T1-weighted arthrogram shows a ''T-sign,'' with leakage of intra-articular contrast material at the undersurface of the UCL at its distal insertion on the sublime tubercle (arrow). (Reprinted, with permission, from: Brunton LM, Anderson MW, Chhabra AB. The elbow. In: Khanna AJ, editor. MRI for orthopaedic surgeons. New York: Thieme; 2010. p 118-28.)

fossae, are best detected on T2-weighted gradient-echo sequences (Figs. 3-A and 3-B). It is important to distinguish loose bodies from osteophytes and synovial hypertrophy, which can mimic them on MRI studies[9]. MRA may prove useful in this setting.

*Ulnar Collateral Ligament Injury*

Injury to the ulnar collateral ligament (UCL) of the elbow (also known as the medial collateral ligament) is common in throwing athletes at all ages and levels of competition[10]. Participation in throwing sports results in repetitive maximal valgus stress applied to the elbow. In addition to UCL injury, this repetitive trauma can lead to posteromedial osteoarthritis, capitellar osteochondral lesions, loose bodies, and/or olecranon stress fractures[11,12]. This constellation of findings in throwing athletes constitutes valgus-extension overload syndrome[12,13].

It is important to distinguish full-thickness and partial-thickness UCL tears and UCL abnormalities from each other and from other causes of medial-sided elbow pain such as ulnar neuropathy, stress fracture, and flexor-pronator mass injury[1,7]. The UCL is normally seen on coronal MRIs as a vertically oriented structure with uniformly low signal intensity coursing between the medial epicondyle and the proximal aspect of the ulna. The UCL is composed of anterior, posterior, and transverse bundles. The anterior bundle is the most important stabilizer against valgus stress and is taut in extension, whereas the posterior bundle is taut in flexion. Consequently, patient positioning with the elbow in extension and the forearm in supination is optimal for the detection of anterior bundle abnormalities by MRI. Although the posterior bundle can be identified on coronal images, it is best traced on axial images as the floor of the cubital tunnel[14]. The transverse bundle bridges the ulnar insertions of the anterior and posterior bundles, but it cannot be readily seen on MRI, and its contribution to elbow stability is unclear.

MRI may easily detect full-thickness tears of the anterior bundle of the UCL. More subtle abnormalities of a partially injured ligament may include attenuation, redundancy, or discontinuity. Increased signal intensity is often found within and adjacent to the ligament on fat-suppressed T2-weighted images, indicating edema and/or hemorrhage[1,15] (Fig. 4-A). Concomitant findings such as adjacent muscle edema and ulnar neuritis are not unusual. MRI is less reliable for detecting partial-thickness tears, but intra-articular contrast agent may improve the sensitivity for detection (Fig. 4-B)[1,16,17]. Timmerman et al.[18] found MRI to be 100% sensitive for full-thickness tears but only 14% sensitive for partial-thickness tears; the specificity was 100%. With intra-articular contrast agent, Schwartz et al.[17] found the sensitivity for partial-thickness tears to be 86%, with 100% specificity. On MRI, the proximal fibers of the anterior bundle can appear stretched and slightly indistinct or splayed, but this finding should not be mistaken for a

Fig. 5-A

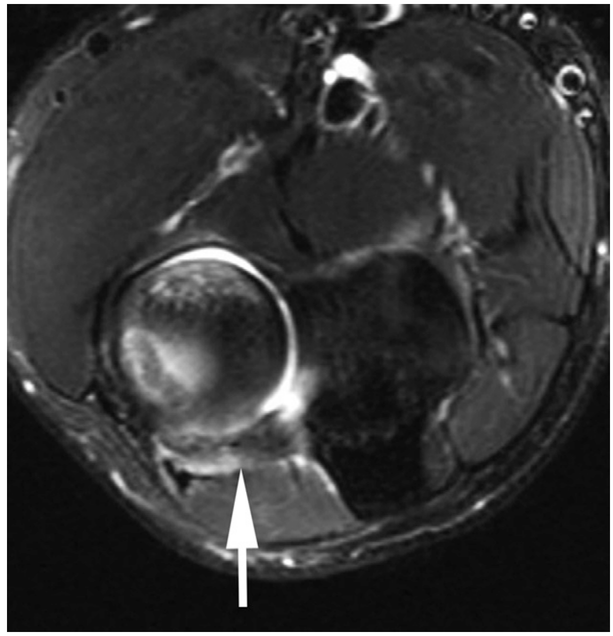

Fig. 5-B

Fig. 5-C

**Figs. 5-A, 5-B, and 5-C** Lateral elbow ligaments. **Fig. 5-A** A normal arthrogram. A coronal fat-suppressed T1-weighted image from an MR arthrogram shows a normal UCL (large arrow) and a normal lateral bundle of the UCL (small arrows). (Adapted from: J Hand Surg Am. 31[6]; Brunton LM, Anderson MW, Pannunzio ME, Khanna AJ, Chhabra AB; Magnetic resonance imaging of the elbow: update on current techniques and indications; p 1001-11; Copyright 2006; with permission from Elsevier.) **Fig. 5-B** A tear of the lateral bundle of the UCL. An axial fat-suppressed T2-weighted image shows thickening and partial tearing of the lateral bundle of the UCL with adjacent high-signal-intensity edema posterior to the radial head (arrow). (Adapted from: J Hand Surg Am. 31[6]; Brunton LM, Anderson MW, Pannunzio ME, Khanna AJ, Chhabra AB; Magnetic resonance imaging of the elbow: update on current techniques and indications; p 1001-11; Copyright 2006; with permission from Elsevier.) **Fig. 5-C** A tear of the lateral collateral ligament complex. A coronal fat-suppressed T2-weighted image (same patient). Note the posterior lateral subluxation of the radial head and associated tear of the lateral collateral ligament complex (arrow).

partial tear[19]. In the pediatric population, the proximal insertion of the anterior bundle can exhibit high signal intensity on fluid-sensitive sequences secondary to higher elastin content compared with adults[20]. The distal ulnar attachment of the anterior bundle has been described as inserting anywhere between 1 mm from the articular margin of the coronoid process[17] and 3 mm distal to the sublime tubercle of the proximal aspect of the ulna[21]. This attachment may create a small recess along the medial margin of the coronoid process on MRA. Consequently, distinguishing between normal anatomy and a pathologic partial undersurface tear at the distal ligament attachment remains challenging[13].

#### Lateral Collateral Ligament Complex Injury

The lateral collateral ligament complex has three main components, all of which represent joint capsule thickenings: the lateral

Fig. 6-A

Fig. 6-B

**Figs. 6-A and 6-B** Biceps tendon rupture. **Fig. 6-A** An axial T2-weighted image shows disruption of the distal aspect of the biceps tendon from its insertion at the radial tuberosity (arrows) and adjacent fluid and soft-tissue edema. (Adapted, with permission, from: Brunton LM, Anderson MW, Chhabra AB. The elbow. In: Khanna AJ, editor. MRI for orthopaedic surgeons. New York: Thieme, 2010. p 118-28.) **Fig. 6-B** A sagittal T2-weighted image shows a completely torn and retracted distal biceps tendon with surrounding high-signal-intensity fluid and soft-tissue edema (arrows). (Adapted from: J Hand Surg Am. 31[6]; Brunton LM, Anderson MW, Pannunzio ME, Khanna AJ, Chhabra AB; Magnetic resonance imaging of the elbow: update on current techniques and indications; p 1001-11; Copyright 2006; with permission from Elsevier.)

bundle of the UCL, the radial collateral ligament, and the annular ligament. The lateral bundle of the UCL is the most posterior structure extending from the lateral humeral epicondyle to the supinator crest of the proximal aspect of the ulna (Fig. 5-A). The radial collateral ligament also arises from the lateral humeral epicondyle, deep to the common extensor tendon origin, and blends with annular ligament fibers surrounding the radial neck. The radial collateral ligament and lateral bundle of the UCL are best visualized on sequential coronal MRI images, but distinguishing them is difficult. Optimally, the image slice thickness should be ≤2 mm[6]. In contrast, the annular ligament is optimally seen on axial and sagittal images[13].

Tears of the lateral collateral ligament complex are common in acute elbow dislocations. The lateral bundle of the UCL is the primary elbow stabilizer with varus stress. Chronic insufficiency of the lateral bundle of the UCL is believed to lead to posterolateral rotatory instability, which is often difficult to diagnose clinically[22]. Identifying lateral collateral ligament complex tears in the setting of chronic instability is challenging on MRI[23]. Terada et al.[24] found that MRI of asymptomatic individuals revealed inconsistent signal characteristics within the lateral bundle of the UCL. Furthermore, 50% of their subjects were excluded because identification of the lateral bundle of the UCL was ambiguous. Potter et al.[8] compared MRIs of asymptomatic and symptomatic individuals with posterolateral rotatory instability. They found that abnormalities of the lateral bundle of the UCL could be detected with three-dimensional gradient-echo and fast-spin-echo sequences in symptomatic patients[8]. MRI findings are similar to those seen in UCL injuries, with combinations of ligament attenuation, redundancy, or discontinuity evident on imaging (Figs. 5-B and 5-C)[15,25]. Acute tears usually involve the proximal ligament attachments[6].

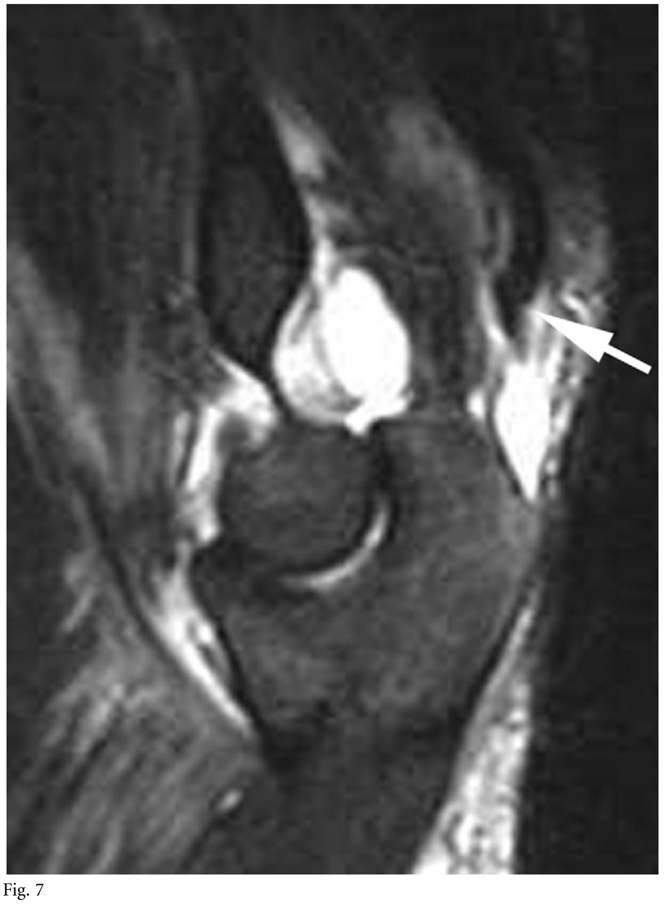

Fig. 7

Triceps tendon tear. A sagittal T2-weighted image reveals a complete tear of the triceps tendon with high-signal-intensity fluid between the olecranon process and the retracted tendon (arrow). (Adapted from: J Hand Surg Am. 31[6]; Brunton LM, Anderson MW, Pannunzio ME, Khanna AJ, Chhabra AB; Magnetic resonance imaging of the elbow: update on current techniques and indications; p 1001-11; Copyright 2006; with permission from Elsevier.)

**Biceps Tendon Injury**

MRI may help distinguish biceps tendinosis, partial tears, and complete tears. Complete rupture typically occurs in men acutely after forced extension of the flexed elbow against a resistive load. A complete rupture is characterized by the absence of low-signal-intensity tendon tissue at the radial tuberosity insertion on axial images (Fig. 6-A). A large amount of high-signal-intensity fluid and/or hemorrhage within the antecubital fossa is often seen on T2-weighted images. Occasionally, a complete rupture can be mistaken for a partial rupture if the bicipital aponeurosis (lacertus fibrosus) tethers the tendon, preventing retraction[13]. The extent of tendon retraction may be assessed on sagittal images; however, since the tendon is obliquely oriented to this plane (Fig. 6-B), the arm may be imaged in elbow flexion, shoulder abduction, and forearm supination to facilitate single-image visualization of the entire biceps tendon[26].

Unlike complete tendon ruptures, partial tears are usually more insidious, often occur secondary to repetitive microtrauma, and may occur in a previously degenerated tendon. Abnormal thickening of the distal aspect of the biceps tendon is often seen on T1-weighted sequences. Increased signal intensity representing tendinopathy and/or a partial intrasubstance tear is seen on T2-weighted sequences. The individual short and long heads comprising the distal portion of the biceps tendon may be separated by linear signal changes and should not be confused with a pathologic tear. Proximally, near the myotendinous junction, the short head of the biceps tendon lies medial to the long head. As the biceps tendon courses distally, the short head travels anteriorly[27]. Occasionally, biceps tendon injury is accompanied by bone marrow edema at the radial tuberosity and increased fluid in the bicipitoradial bursa[25,28].

**Triceps Tendon Injury**

Complete triceps tendon tears are typically traumatic and clinically appear with the inability to extend the elbow against gravity. MRI is used when clinical findings are equivocal. A complete rupture of the tendon typically involves avulsion from the olecranon. Often, an osseous avulsion fragment may be appreciated on radiographs. T2-weighted sequences will show extensive edema adjacent to the triceps. The extent of tendon retraction may be evaluated on sagittal T1-weighted sequences (Fig. 7)[15,25]. Tendon thickening or thinning resulting from partial rupture and/or tendinopathy is best appreciated on T1-weighted sequences. Focal areas of increased signal within the tendon or associated olecranon bursitis may be evident on T2-weighted sequences.

## *Degenerative Conditions*

**Lateral Epicondylitis**

Lateral epicondylitis, or "tennis elbow," is the most common elbow overuse disorder. The term "epicondylitis" may be a misnomer because mucoid degeneration and microtears of the extensor carpi radialis brevis tendon origin, rather than acute inflammation, are the dominant pathologic features[12,29]. In recalcitrant disease, MRI may rule out concomitant causes of elbow pain such as osteoarthritis, osteochondritis dissecans, radial tunnel syndrome, posterolateral rotatory instability, occult fracture, and/or loose bodies[1,30]. Lateral collateral ligament complex abnormalities are not unusual in severe cases of lateral epicondylitis (Figs. 8-A and 8-B)[31].

Abnormally high signal intensity in a thickened common extensor tendon origin on T2-weighted and STIR sequences is the typical finding of isolated lateral epicondylitis. If the common extensor tendon itself appears normal, adjacent soft-tissue edema usually predominates on T2-weighted sequences[15,25]. MRI has 90% to 100% sensitivity and 83% to 100% specificity for detecting epicondylitis[32].

**Medial Epicondylitis**

MRI is not commonly used for diagnosing medial epicondylitis. Rather, MRI may be useful in cases of refractory medial epicondylar pain to exclude UCL injury or ulnar neuritis[13]. On T1-weighted sequences, a thickened common flexor tendon origin may be seen. On T2-weighted sequences, partial tendon

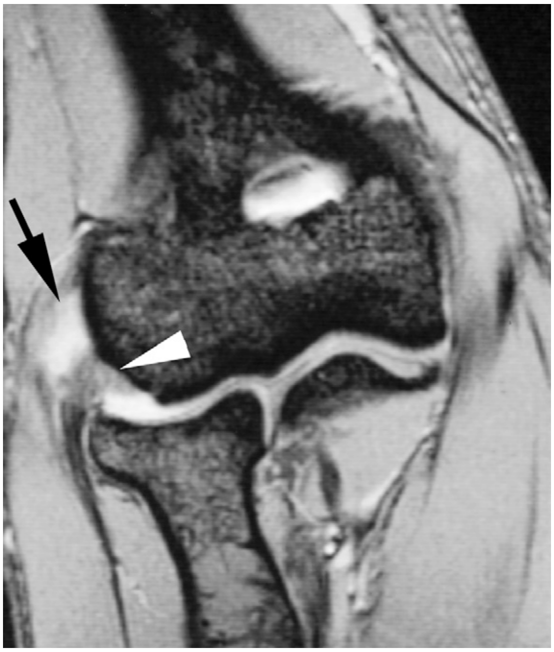

Fig. 8-A

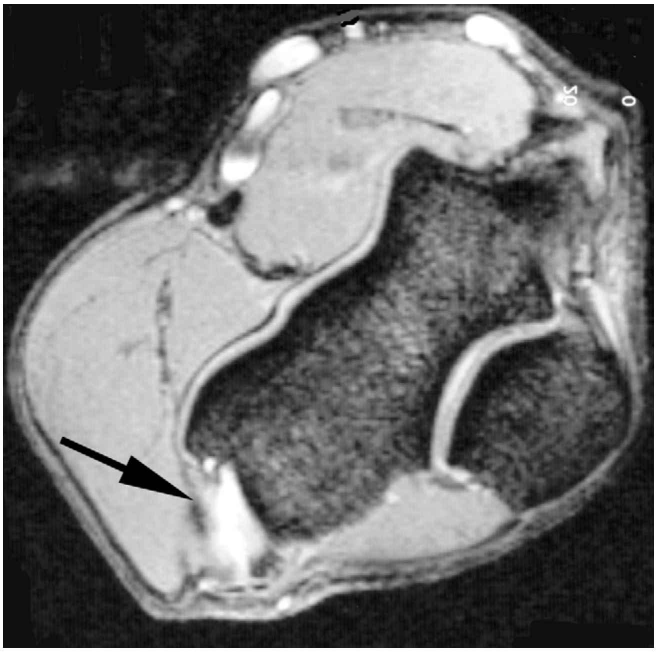


Fig. 8-B

**Figs. 8-A and 8-B** Lateral epicondylitis. **Fig. 8-A** A coronal gradient-echo T2-weighted image of the right elbow shows prominent partial tearing of the common extensor tendon (arrow) with partial tearing of the underlying radial collateral ligament as well (arrowhead). (Adapted from: J Hand Surg Am. 31[6]; Brunton LM, Anderson MW, Pannunzio ME, Khanna AJ, Chhabra AB; Magnetic resonance imaging of the elbow: update on current techniques and indications; p 1001-11; Copyright 2006; with permission from Elsevier.) **Fig. 8-B** An axial gradient-echo T2-weighted image (same patient) again shows extensive tearing within the common extensor tendon at its origin (arrow).

Fig. 9-A

Fig. 9-B

**Figs. 9-A and 9-B** Medial epicondylitis. **Fig. 9-A** A coronal T1-weighted image shows abnormal intermediate signal intensity within the common flexor tendon at its origin (arrow). **Fig. 9-B** A coronal fat-saturated T2-weighted image reveals focal partial tearing of the tendon (arrow).

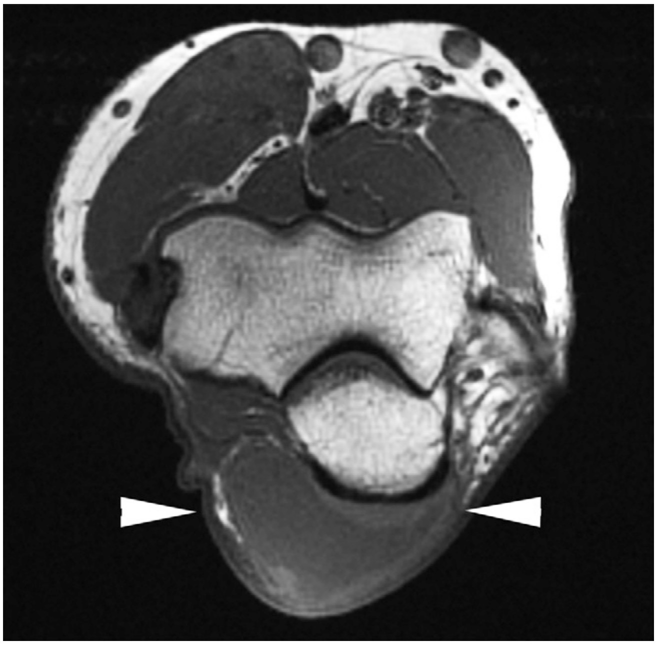

Fig. 10-A

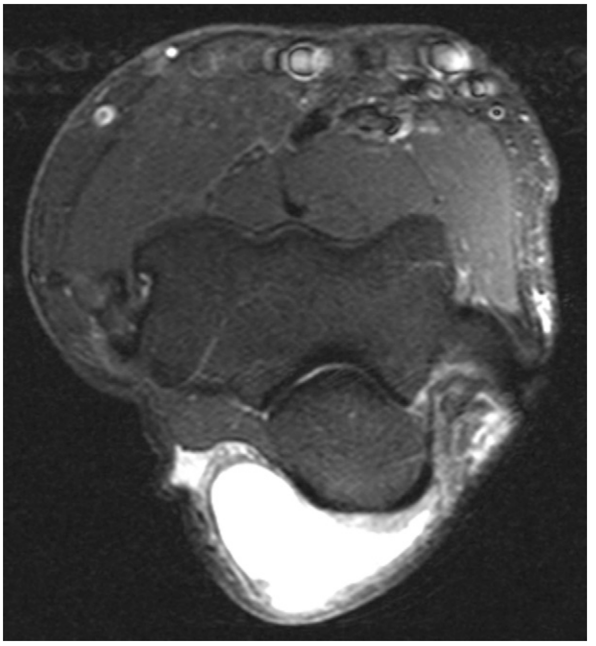

Fig. 10-B

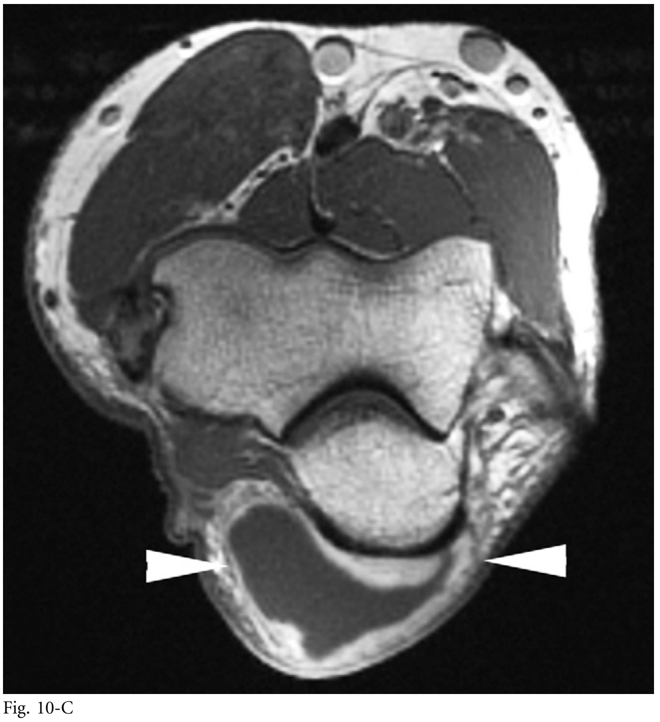

Fig. 10-C

**Figs. 10-A, 10-B, and 10-C** Olecranon bursitis. **Fig. 10-A** An axial T1-weighted image of an inflamed olecranon bursa (arrowheads). **Fig. 10-B** An axial fat-suppressed T2-weighted image of the same inflamed olecranon bursa. **Fig. 10-C** An axial T1-weighted image after the intravenous injection of gadolinium contrast agent shows peripheral enhancement of the inflamed synovium (arrowheads) and no enhancement of the central fluid. Note the lack of high-signal-intensity fluid within the underlying joint.

tearing and/or local soft-tissue edema may be appreciated (Figs. 9-A and 9-B). This disease usually involves the flexor carpi radialis and pronator teres tendons[13].

## *Infectious Conditions*

### Septic Arthritis

The elbow is involved in 3% to 13% of all septic arthritis cases[33]. MRI can help distinguish a joint effusion from superficial cellulitis or bursitis (Figs. 10-A, 10-B, and 10-C). Joint effusion and synovitis are manifested by low signal intensity on T1-weighted images and high signal intensity on T2-weighted images. MRI cannot characterize intra-articular fluid as normal, hemoarthrotic, or purulent. Synovial hyperemia and swelling with shaggy enhancement of the rim may be seen on gadolinium-enhanced T1-weighted images[7]. The addition of intravenous gadolinium contrast agent facilitates localization of

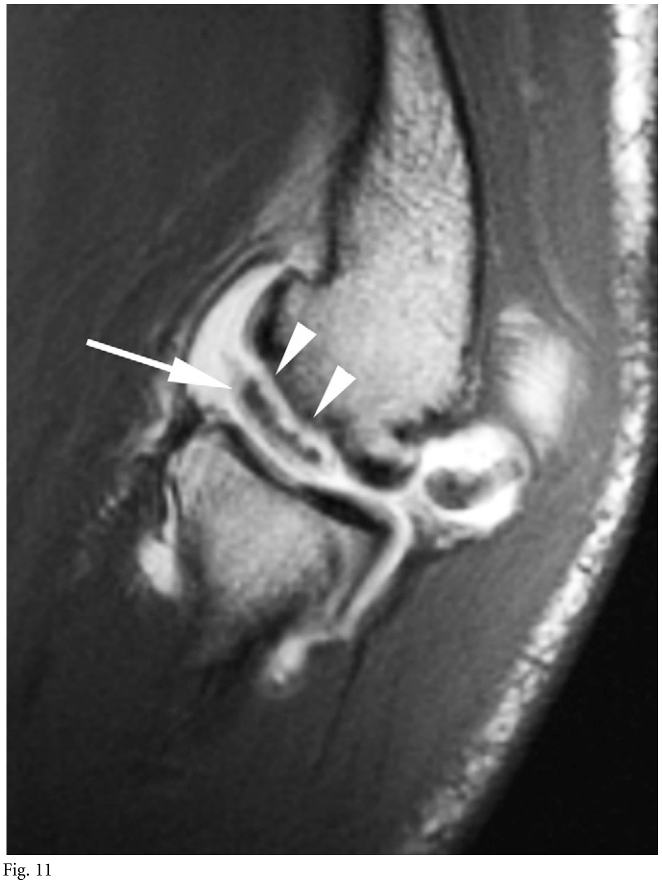

Fig. 11
Osteochondral lesion of the capitellum. A sagittal T1-weighted image from an MR arthrogram reveals an osteochondral lesion of the capitellum with a large osteochondral fragment (arrow). The high-signal-intensity gadolinium between it and the underlying bone (arrowheads) indicates an unstable fragment.

focal adjacent soft-tissue abscesses that may require surgical incision and drainage[34].

**Osteomyelitis**

MRI is the best modality for evaluating bone involvement in cases of infection around the elbow. Acute osteomyelitis generates inflammation of medullary bone detectable by MRI well before findings are evident on radiographs. T1-weighted images show confluent low signal intensity contrasting with surrounding bright normal marrow. STIR or fat-suppressed T2-weighted images are the most sensitive for infection; affected areas appear with high signal intensity. Correlation with the patient history and physical examination are important because findings may mimic neoplasms or osteonecrosis[35].

## *Other Conditions*

**Osteochondritis Dissecans**

Osteochondritis dissecans is an idiopathic articular cartilage disorder affecting adolescents with a history of repetitive elbow overuse. Osteochondritis dissecans is commonly encountered at the lateral distal aspect of the humerus, where the convex surface of the capitellum is most vulnerable. The clinician should be aware of the possibility of a capitellum pseudodefect, which appears as a notch at the junction of the lateral humeral condyle and the posterior capitellum on coronal images. This anatomic variant may be confused with an osteochondral lesion; however, its smooth contour, absence of bone marrow edema, and posterior location are distinguishing features[13,27,36]. The trochlear groove, a focal area devoid of cartilage at the junction of the coronoid and olecranon articular surfaces of the ulna in the trochlear notch, may also be confused with an osteochondral lesion. The groove is most apparent on sagittal images and will lack the bone marrow edema characteristic of osteochondritis dissecans[4].

In the acute phase of osteochondritis dissecans, a joint effusion is often present. In early stages, the capitellum may show subtle changes on radiographs that are more apparent on MRI. Focal areas of subchondral low signal intensity on T1-weighted images are characteristic. Fat-suppressed T2-weighted images are the most sensitive for evaluating osteochondral lesions at the capitellar surface; however, they are also the least specific. When the clinical suspicion is high, a fat-suppressed T2-weighted image can be used as a “screening” examination and then correlated with the T1-weighted image.

In patients less than twelve years old, the radiographic findings, sometimes termed Panner disease, are often self-limiting. For older patients, however, articular cartilage deterioration may progress, with a crack propagating between the subchondral plane and the underlying bone, ultimately generating a loose body when the fragment becomes unstable[13]. MRI is perhaps most useful for determining an osteochondral fragment’s stability and viability. Instability is characterized by fluid tracking behind the fragment on fat-suppressed T2-weighted images and contrast material surrounding the fragment on MRA (Fig. 11). Fragment enhancement after intravenous gadolinium contrast agent administration suggests adequate blood supply and bone viability[37].

**Compression Neuropathies**

Common compression neuropathies at the elbow include cubital tunnel, radial tunnel, posterior interosseous nerve, and pronator syndromes. Electromyography and nerve conduction studies are the most frequently used adjunctive diagnostic tests. MRI is used when nonoperative management fails or the neuropathy recurs after surgical intervention. Major peripheral nerves may be traced on sequential axial images and appear isointense compared with muscle[27]. The ulnar nerve is normally located within the cubital tunnel posterior to the medial humeral epicondyle and accompanied by perineural fat. The paucity of perineural fat makes the median nerve difficult to visualize[13], but anatomically the nerve lies medial to the biceps tendon and brachial artery or between the superficial and deep heads of the pronator teres distally[36]. The radial nerve may be identified proximally near the lateral head of the triceps before coursing between the brachioradialis and brachialis muscles[38] or distally bifurcating into the posterior interosseous nerve and superficial sensory branch at the proximal border of the supinator muscle[13].

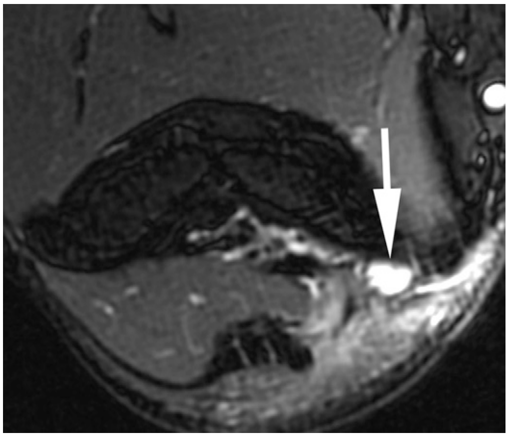

Fig. 12-A

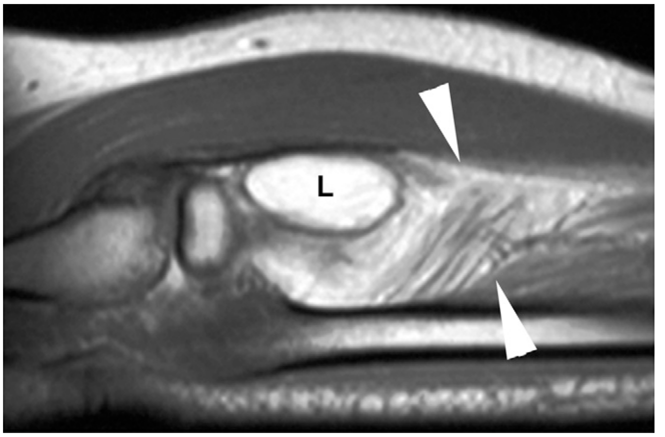


Fig. 12-B

**Figs. 12-A and 12-B** Nerve pathology. **Fig. 12-A** Ulnar neuritis. An axial STIR image shows a markedly enlarged ulnar nerve and increased signal intensity (arrow), consistent with nerve inflammation. **Fig. 12-B** Denervated muscle from compression neuropathy. A sagittal T1-weighted image reveals a lipoma (L) within the supinator muscle and fatty atrophy affecting the adjacent extensor muscles (arrowheads) from long-standing compression of the posterior interosseous nerve by the lipoma. (Adapted from: J Hand Surg Am. 31[6]; Brunton LM, Anderson MW, Pannunzio ME, Khanna AJ, Chhabra AB; Magnetic resonance imaging of the elbow: update on current techniques and indications; p 1001-11; Copyright 2006; with permission from Elsevier.)

MRI has the greatest utility for assessing cubital tunnel syndrome, especially in equivocal or recurrent cases. Vucic et al.[39] suggested that MRI may be more sensitive than nerve conduction studies in diagnosing ulnar neuropathy at the elbow. MRI findings in compression neuropathy may include nerve thickening, an adjacent space-occupying lesion, or constricting anatomy on T1-weighted sequences. Common sites of compression include the arcade of Struthers, the medial head of the triceps, the ligament of Osborne, and the deep flexor pronator aponeurosis[12]. A mottled nerve appearance or perineural edema on T2-weighted sequences may represent inflammation (Fig. 12-A) indicative of ulnar neuritis. Chronic neuropathy may show adjacent muscle denervation with atrophy and/or fatty infiltration on T1-weighted images (Fig. 12-B) or muscle edema on T2-weighted images[40].

### Synovial Disorders

MRI may aid in the diagnosis of inflammatory arthritides, crystal deposition disorders, pigmented villonodular synovitis, and idiopathic synovial osteochondromatosis[25]. MRI is a powerful tool for detecting early inflammatory arthritides, such as rheumatoid arthritis. Intravenous gadolinium contrast agent produces striking enhancement of proliferative synovium (pannus). Periarticular erosions secondary to pannus may be more apparent on MRI than on radiographs. Pigmented villonodular synovitis has a unique MRI appearance on gradient-echo imaging, showing accentuated "signal dropout" secondary to hemosiderin deposition in areas of involvement. Other nonspecific MRI findings of pigmented villonodular synovitis include variable synovial proliferation and joint effusion[41,42]. Synovial osteochondromatosis results in numerous osteocartilaginous nodules within joints, bursae, or tendon sheaths. Nonosseous synovial lesions are isointense or slightly hyperintense compared with muscle on T1-weighted and T2-weighted images[7]. If these lesions are calcified, signal voids are seen within chondroid masses on all sequences.

### Soft-Tissue Masses

MRI is the standard modality for evaluating equivocal elbow soft-tissue masses. Intravenous contrast agent administration


Fig. 13

Lipoma. An axial T1-weighted image shows the similarity in signal intensity between the well-circumscribed lipoma (L) and the adjacent subcutaneous fat. (Reprinted, with permission, from: Brunton LM, Anderson MW, Chhabra AB. The elbow. In: Khanna AJ, editor. MRI for orthopaedic surgeons. New York: Thieme, 2010. p 118-128.)

helps differentiate solid from cystic lesions and may aid in distinguishing certain tumors. Determinate lesions are soft-tissue masses that can be identified by MRI characteristics, and include lymph nodes, lipomas, ganglia, hemangiomas, neurofibromas, pigmented villonodular synovitis, and synovial osteochondromatosis[5,43].

An enlarged medial epitrochlear node may be mistaken on MRI for a more aggressive lesion, leading to unnecessary excisional biopsy in some scenarios[27]. The node enlargement may be associated with rheumatoid arthritis, lupus, cat scratch disease, tuberculosis, lymphoproliferative disorders, or (rarely) metastatic disease[44,45]. Tumoral lymph nodes are usually rounded and well defined, with less soft-tissue edema and stranding compared with lymph nodes in patients with infection.

Lipomas are well-circumscribed masses that match the signal intensity of subcutaneous fat on all sequences. Fat-suppression sequences show homogenous suppression of the suspected mass. Lipomas are usually located subcutaneously with a thin surrounding capsule but may occur within muscle as a more infiltrative mass (Fig. 13).

Ganglia are another type of determinate elbow lesion. However, most are diagnosed clinically without MRI. Defined margins, a spherical shape, and an occasional multilocular appearance may be appreciated. Peripheral enhancement with intravenous contrast agent is characteristic.

Cavernous hemangiomas are well-circumscribed lobulated masses that appear isointense compared with muscle on T1-weighted sequences and contain areas of high signal intensity from interspersed fat. T2-weighted sequences appear heterogeneously hyperintense because of pooled blood in larger vessels. In the case of a high-flow vascular malformation, large feeding and draining vessels show dark “flow voids” related to fast-flowing blood.

Neurofibromas produce fusiform nerve enlargement on T1-weighted sequences. The tumor infiltrates the nerve fascicles, typically those of smaller cutaneous nerves. MRI sequences perpendicular to the nerve course show the tumor location relative to the fascicles.

Masses that do not show classic MRI features of one of the above-listed lesions should be considered “indeterminate,” and consideration should be given to obtaining a fine needle aspiration or open biopsy[43].

## Conclusion

MRI is a valuable, noninvasive method of evaluating a wide variety of conditions involving the elbow. There are various MRI techniques and characteristic findings that allow the orthopaedic surgeon to recognize and diagnose many pathologic elbow conditions. ■

Ashvin K. Dewan, MD
A. Jay Khanna, MD, MBA
c/o Elaine P. Henze, BJ, ELS,
Medical Editor and Director, Editorial Services,
Department of Orthopaedic Surgery,
The Johns Hopkins University/Johns
Hopkins Bayview Medical Center,
4940 Eastern Avenue #A665,
Baltimore, MD 21224.
E-mail address: ehenze1@jhmi.edu

A. Bobby Chhabra, MD
Mark W. Anderson, MD
Departments of Orthopaedic Surgery (A.B.C.)
and Radiology (M.W.A.),
University of Virginia, 1827 University Avenue,
Charlottesville, VA 22904

Lance M. Brunton, MD
Excela Health Orthopaedics and Sports Medicine,
8775 Norwin Avenue,
North Huntingdon, PA 15642

## References

1. Brunton LM, Anderson MW, Chhabra AB. The elbow. In: Khanna AJ, editor. MRI for orthopaedic surgeons. New York: Thieme; 2010. p 118-28.
2. O’Dwyer H, O’Sullivan P, Fitzgerald D, Lee MJ, McGrath F, Logan PM. The fat pad sign following elbow trauma in adults: its usefulness and reliability in suspecting occult fracture. J Comput Assist Tomogr. 2004 Jul-Aug;28(4):562-5.
3. Skaggs DL, Mirzayan R. The posterior fat pad sign in association with occult fracture of the elbow in children. J Bone Joint Surg Am. 1999 Oct;81(10):1429-33.
4. Stein JM, Cook TS, Simonson S, Kim W. Normal and variant anatomy of the elbow on magnetic resonance imaging. Magn Reson Imaging Clin N Am. 2011 Aug;19(3):609-19.
5. Griffith JF, Roebuck DJ, Cheng JCY, Chan YL, Rainer TH, Ng BKW, Metreweli C. Acute elbow trauma in children: spectrum of injury revealed by MR imaging not apparent on radiographs. AJR Am J Roentgenol. 2001 Jan;176(1):53-60.
6. Kaplan LJ, Potter HG. MR imaging of ligament injuries to the elbow. Radiol Clin North Am. 2006 Jul;44(4):583-94, ix.
7. Jbara M, Patnana M, Kazmi F, Beltran J. MR imaging: arthropathies and infectious conditions of the elbow, wrist, and hand. Magn Reson Imaging Clin N Am. 2004 May;12(2):361-79, vii.
8. Potter HG, Weiland AJ, Schatz JA, Paletta GA, Hotchkiss RN. Posterolateral rotatory instability of the elbow: usefulness of MR imaging in diagnosis. Radiology. 1997 Jul;204(1):185-9.
9. Potter HG. Imaging of posttraumatic and soft tissue dysfunction of the elbow. Clin Orthop Relat Res. 2000 Jan;370:9-18.
10. Cain EL Jr, Dugas JR, Wolf RS, Andrews JR. Elbow injuries in throwing athletes: a current concepts review. Am J Sports Med. 2003 Jul-Aug;31(4):621-35.
11. Lynch JR, Waitayawinyu T, Hanel DP, Trumble TE. Medial collateral ligament injury in the overhand-throwing athlete. J Hand Surg Am. 2008 Mar;33(3):430-7.
12. Stevens KJ. Magnetic resonance imaging of the elbow. J Magn Reson Imaging. 2010 May;31(5):1036-53.
13. Stevens KJ, McNally EG. Magnetic resonance imaging of the elbow in athletes. Clin Sports Med. 2010 Oct;29(4):521-53.
14. Fowler KAB, Chung CB. Normal MR imaging anatomy of the elbow. Radiol Clin North Am. 2006 Jul;44(4):553-67, viii.
15. Fritz RC, Steinbach LS. Magnetic resonance imaging of the musculoskeletal system: Part 3. The elbow. Clin Orthop Relat Res. 1996 Mar;324:321-39.
16. Hill NB Jr, Bucchieri JS, Shon F, Miller TT, Rosenwasser MP. Magnetic resonance imaging of injury to the medial collateral ligament of the elbow: a cadaver model. J Shoulder Elbow Surg. 2000 Sep-Oct;9(5):418-22.
17. Schwartz ML, Al-Zahrani S, Morwessel RM, Andrews JR. Ulnar collateral ligament injury in the throwing athlete: evaluation with saline-enhanced MR arthrography. Radiology. 1995 Oct;197(1):297-9.
18. Timmerman LA, Schwartz ML, Andrews JR. Preoperative evaluation of the ulnar collateral ligament by magnetic resonance imaging and computed tomography

arthrography. Evaluation in 25 baseball players with surgical confirmation. Am J Sports Med. 1994 Jan-Feb;22(1):26-31; discussion 32.

**19.** Fowler KAB, Chung CB. Normal MR imaging anatomy of the elbow. Magn Reson Imaging Clin N Am. 2004 May;12(2):191-206, v.

**20.** Sugimoto H, Ohsawa T. Ulnar collateral ligament in the growing elbow: MR imaging of normal development and throwing injuries. Radiology. 1994 Aug;192(2):417-22.

**21.** Munshi M, Pretterklieber ML, Chung CB, Haghighi P, Cho JH, Trudell DJ, Resnick D. Anterior bundle of ulnar collateral ligament: evaluation of anatomic relationships by using MR imaging, MR arthrography, and gross anatomic and histologic analysis. Radiology. 2004 Jun;231(3):797-803. Epub 2004 Apr 22.

**22.** O'Driscoll SW, Bell DF, Morrey BF. Posterolateral rotatory instability of the elbow. J Bone Joint Surg Am. 1991 Mar;73(3):440-6.

**23.** Grafe MW, McAdams TR, Beaulieu CF, Ladd AL. Magnetic resonance imaging in diagnosis of chronic posterolateral rotatory instability of the elbow. Am J Orthop (Belle Mead NJ). 2003 Oct;32(10):501-3; discussion 504.

**24.** Terada N, Yamada H, Toyama Y. The appearance of the lateral ulnar collateral ligament on magnetic resonance imaging. J Shoulder Elbow Surg. 2004 Mar-Apr;13(2):214-6.

**25.** Melloni P, Valls R. The use of MRI scanning for investigating soft-tissue abnormalities in the elbow. Eur J Radiol. 2005 May;54(2):303-13.

**26.** Giuffrè BM, Moss MJ. Optimal positioning for MRI of the distal biceps brachii tendon: flexed abducted supinated view. AJR Am J Roentgenol. 2004 Apr;182(4):944-6.

**27.** Sampaio ML, Schweitzer ME. Elbow magnetic resonance imaging variants and pitfalls. Magn Reson Imaging Clin N Am. 2010 Nov;18(4):633-42. Epub 2010 Sep 01.

**28.** Williams BD, Schweitzer ME, Weishaupt D, Lerman J, Rubenstein DL, Miller LS, Rosenberg ZS. Partial tears of the distal biceps tendon: MR appearance and associated clinical findings. Skeletal Radiol. 2001 Oct;30(10):560-4.

**29.** Kraushaar BS, Nirschl RP. Tendinosis of the elbow (tennis elbow). Clinical features and findings of histological, immunohistochemical, and electron microscopy studies. J Bone Joint Surg Am. 1999 Feb;81(2):259-78.

**30.** Aoki M, Wada T, Isogai S, Kanaya K, Aiki H, Yamashita T. Magnetic resonance imaging findings of refractory tennis elbows and their relationship to surgical treatment. J Shoulder Elbow Surg. 2005 Mar-Apr;14(2):172-7.

**31.** Bredella MA, Tirman PFJ, Fritz RC, Feller JF, Wischer TK, Genant HK. MR imaging findings of lateral ulnar collateral ligament abnormalities in patients with lateral epicondylitis. AJR Am J Roentgenol. 1999 Nov;173(5):1379-82.

**32.** Miller TT, Shapiro MA, Schultz E, Kalish PE. Comparison of sonography and MRI for diagnosing epicondylitis. J Clin Ultrasound. 2002 May;30(4):193-202.

**33.** Schweitzer M, Morrison WB. Arthropathies and inflammatory conditions of the elbow. Magn Reson Imaging Clin N Am. 1997 Aug;5(3):603-17.

**34.** Berquist TH, Broderick DF. Musculoskeletal infection. In: Berquist TH, editor. MRI of the Musculoskeletal System. 5th ed. Philadelphia: Lippincott Williams & Wilkins; 2006. pp916-47.

**35.** Boutin RD, Brossmann J, Sartoris DJ, Reilly D, Resnick D. Update on imaging of orthopedic infections. Orthop Clin North Am. 1998 Jan;29(1):41-66.

**36.** Simonson S, Lott K, Major NM. Magnetic resonance imaging of the elbow. Semin Roentgenol. 2010 Jul;45(3):180-93.

**37.** Kijowski R, De Smet AA. MRI findings of osteochondritis dissecans of the capitellum with surgical correlation. AJR Am J Roentgenol. 2005 Dec;185(6):1453-9.

**38.** Rosenberg ZS, Bencardino J, Beltran J. MR features of nerve disorders at the elbow. Magn Reson Imaging Clin N Am. 1997 Aug;5(3):545-65.

**39.** Vucic S, Cordato DJ, Yiannikas C, Schwartz RS, Shnier RC. Utility of magnetic resonance imaging in diagnosing ulnar neuropathy at the elbow. Clin Neurophysiol. 2006 Mar;117(3):590-5. Epub 2006 Feb 14.

**40.** Kijowski R, Tuite M, Sanford M. Magnetic resonance imaging of the elbow. Part I: normal anatomy, imaging technique, and osseous abnormalities. Skeletal Radiol. 2004 Dec;33(12):685-97. Epub 2004 Oct 05.

**41.** Cheng XG, You YH, Liu W, Zhao T, Qu H. MRI features of pigmented villonodular synovitis (PVNS). Clin Rheumatol. 2004 Feb;23(1):31-4. Epub 2004 Jan 09.

**42.** Khanna AJ, Cosgarea AJ, Mont MA, Andres BM, Domb BG, Evans PJ, Bluemke DA, Frassica FJ. Magnetic resonance imaging of the knee. Current techniques and spectrum of disease. J Bone Joint Surg Am. 2001;83 (Suppl 2 Pt 2):128-41.

**43.** Frassica FJ, Khanna JA, McCarthy EF. The role of MR imaging in soft tissue tumor evaluation: perspective of the orthopedic oncologist and musculoskeletal pathologist. Magn Reson Imaging Clin N Am. 2000 Nov;8(4):915-27.

**44.** Gielen J, Wang XL, Vanhoenacker F, De Schepper H, De Beuckeleer L, Vandevenne J, De Schepper A. Lymphadenopathy at the medial epitrochlear region in cat-scratch disease. Eur Radiol. 2003 Jun;13(6):1363-9. Epub 2002 Oct 02.

**45.** Selby CD, Marcus HS, Toghill PJ. Enlarged epitrochlear lymph nodes: an old physical sign revisited. J R Coll Physicians Lond. 1992 Apr;26(2):159-61.